Ionizing Radiation Effects on Non Volatile Read Only Memory Cells

Sebania Libertino, Domenico Corso, Michael Lisiansky, Yakov Roizin, Felix Palumbo, Fabio Principato, Calogero Pace, Paolo Finocchiaro, and Salvatore Lombardo

***Abstract*—Threshold voltage ($V_{\rm th}$) and drain-source current ($I_{\rm DS}$) behaviour of nitride read only memories (NROM) were studied both in situ during irradiation or after irradiation with photons and ions. $V_{\rm th}$ loss fluctuations are well explained by the same Weibull statistics regardless of the irradiation species and total dose. Results of drain current measurements in-situ during irradiation with photons and ions reveal a step-like increase of $I_{\rm DS}$ with the total irradiation dose. A brief physical explanation is also provided.**

***Index Terms*—Flash memories, nitride read-only memories (NROM), oxide/nitride/oxide (ONO), radiation hardness.**

I. Introduction

MOST of the commercial semiconductor nonvolatile memory cells are based on charge storage in floating gates (FG) of MOS structures. The retention of the stored charge in these devices is limited by the intrinsic leakage currents through the dielectrics. Fig. 1(a) schematically describes the cross-section of polysilicon FG memory structure. It also explains the electron loss from the FG if a leakage path is created in the bottom oxide. All the FG charge escapes through the leakage path and a full memory discharge is achieved in a relatively short time. A successful alternative to the FG memory architecture is provided by the use of discrete nodes for charge storage. This approach is also based on a MOS transistor with a FG but employs discrete storage of charge on traps in thin dielectric layers. The two most studied examples, also reported in Fig. 1. Silicon nanocrystals (NC) embedded in a high-quality oxide layer (Fig. 1(b) or silicon/oxide/nitride/oxide/silicon (SONOS) structures with stoichiometric or silicon rich $\mathrm{Si_3N_4}$ Fig. 1(c) are employed (in particular in nitride read-only memories, NROM). In the last example (NROM) the charge is stored on silicon nitride traps. The discrete storage devices allow enhanced reliability since the charge is stored at numerous trapping nodes and cannot flow laterally. If a defect is formed in the FG surrounding dielectric, the charge loss is limited only to one or few nodes closest to the defect. The remaining nodes maintain their charge state and thus the information is preserved (see Fig. 1(b) and (c) for NC and NROM structures, respectively). In particular, if the leakage path is not created where the charge is stored (see Fig. 1(c)) no discharge occurs.

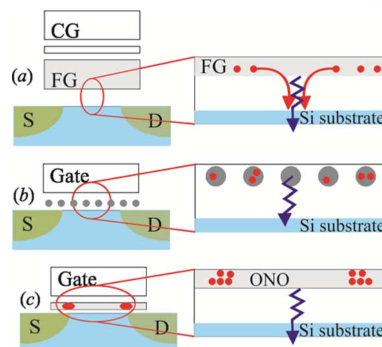

Fig. 1. Schematic view of the device cross-section for: (a) FG, (b) NC, (c) NROM memory cells. The bit discharge mechanisms are schematically shown on the right side of each device schematic.

Ionizing radiation has a pronounced effect on the charge trapped in the memory cell. Many different memory principles and architectures were tested for ionizing radiation hardness assessment. Radiation immunity of polysilicon FG memory devices [1], NC [2] and, more recently, NROM [3], [4] memories have been widely studied. The features of a NROM device are shown in Fig. 2. The memory bit is programmed by channel-hot-electron (CHE) injection. The trapped charge package is strongly localized in regions of ~ 20–40 nm in length [5], [6] at the transistor channel edges. The read operation is performed by applying a low voltage in the opposite direction with respect to the programming current (see Fig. 2(a), arrows for programming and reading). The strong localization allows one to program also the other end of the channel as an independent bit, thus allowing the storage of two bits per cell (Fig. 2(b)) [3].

Typical $I_{\rm DS}-V_G$ transcharacteristics for bit 1 are shown in Fig. 3 for the different device states: fresh (dot-dashed black line), programmed (blue solid line) and erased (dotted red line).

Manuscript received July 12, 2012; revised September 05, 2012; accepted September 12, 2012. Date of publication October 25, 2012; date of current version December 11, 2012. This work was supported by “con il contributo del Ministero degli Affari Esteri, Direzione Generale per la Promozione del Sistema Paese” through the Progetto di Grande Rilevanza Italia—Argentina “Caratterizzazione durante e post-irraggiamento di dispositivi microelettronici per applicazioni avioniche o spaziali.”.

S. Libertino. D. Corso, and S. Lombardo are with the Istituto per la microelettronica e microsistemi (IMM) of the National Council of Research (CNR), 95121 Catania, Italy (e-mail: sebania.libertino@imm.cnr.it).

M. Lisiansky, Y. Roizin are with Tower Semiconductor, Migdal Haemek, 23105, Israel (e-mail: michaelx@towersemi.com).

F. Palumbo is with the Consejo Nacional de Investigaciones Científicas y Técnicas—Comision Nacional de Energia Atomica (CONICET-CNEA), 1650 Buenos Aires, Argentina (e-mail: palumbo@cnea.gov.ar).

F. Principato is with Department of Physics, University of Palermo, 90128 Palermo, Italy (e-mail: fabio.principato@unipa.it).

C. Pace is with Department of Electronics, Computer Science and Systems, University of Calabria, Rende (CS), Italy (e-mail: cpace@unical.it).

P. Finocchiaro is with INFN Laboratori Nazionali del Sud, 95100 Catania, Italy (e-mail: finocchiaro@lns.infn.it).

Color versions of one or more of the figures in this paper are available online at http://ieeexplore.ieee.org.

Digital Object Identifier 10.1109/TNS.2012.2219071

0018-9499/$31.00 © 2012 IEEE

TABLE I
LIST OF THE SPECIES IRRADIATED AND DETAILS OF IRRADIATION (WHERE APPLICABLE): ENERGY, DOSE (Φ), DOSE RATE, PROJECTED RANGE (R_p), STRAGGLING (ΔR_p), LINEAR ENERGY TRANSFER (LET) AND ABSORBED DOSE ($\mathrm{DOSE_{ABS}}$) IN krad (SI)

Species	E [MeV]	Φ [cm^{-2}]	Dose rate	Rp [µm]	ΔRp [µm]	LET [MeV/mg/cm^2]	*DOSE$_{abs}$* [krad(Si)]
γ-rays (^{60}Co)	~1.25	-	3.6 rad(Si)/s	-	-	-	9.4–52
X-rays (W–L lines)	~0.010	-	3.9 rad(Si)/s	-	-	-	3–100
^{11}*B*	10	10^8–5×10^{10}		12	0.2	3.5	5.8-2900
^{79}*Br*	196	5×10^8–10^{11}		26.4	0.6	38.8	255-51040
^{197}*Au*	5100	10^9–5×10^{10}		291	1.1	64.4	1200-60190

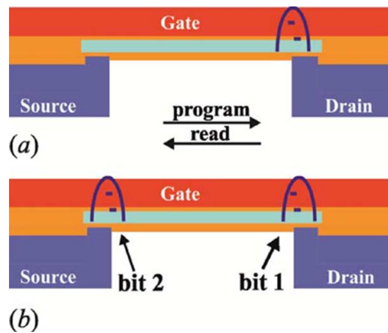

Fig. 2. Schematic view of device operation: (a) the charge is stored at the junction edge and the programming/reading conditions (arrows) for bit 1 are also indicated; (b) the possibility to store two bits per cell is schematically shown. Different colors represent different materials: dark blue for Si, orange for Si oxide, light blue for silicon nitride.

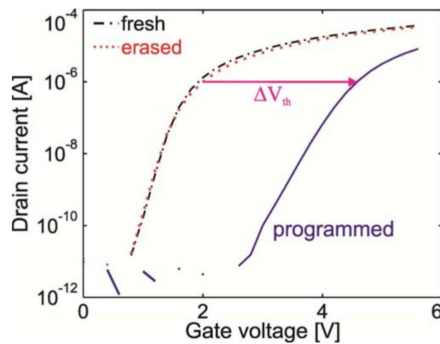

Fig. 3. Drain-source current as a function of the gate voltage for a fresh bit (black dot-dashed line), after programmed (blue solid line), after erase (red dotted line). The arrow indicates the threshold voltage shift.

The threshold voltage ($V_{\rm th}$) here is defined as the gate voltage at $I_{\rm DS} = 1\ \mu$A. A clear $V_{\rm th}$ increase is evident in Fig. 3 for the programmed cell with respect to the "fresh" state. The erase operation is performed by band-to-band tunneling assisted hot hole injection. Also holes are locally injected into the regions close to the metallurgical junctions, where the electron charge is stored. As a result of the erase operation, the device I-V curve returns to the "fresh" state.

NROM memories are a very promising candidate for radiation hardness applications thanks to the strong localization of the charge [7]. In fact, since the volume where the charge is trapped is very small (even if there are two programmed bits), the probability of creating a leakage path in such volume is low. Moreover, even if a leakage path is created, only a very limited number of trapped charge carriers are lost: in NROM, unlike in polycrystalline Si FG memories, lateral charge migration is strongly suppressed. For moderate total absorbed doses (e.g., below 100 krad(Si) of γ-radiation) the main degradation effect is trapping of holes generated by ionizing radiation within, or in the proximity of ONO [3]. Trapping of positive charge leads to the $V_{\rm th}$ loss. In this paper we present the statistics of $V_{\rm th}$ loss of NROM single memory cells after irradiation with photons or heavy ions.

The understanding of the discharge mechanism could help in the design of radiation hard systems. In fact, the possibility to model the discharge mechanism could allow one to implement a memory reprogramming algorithm to improve the system radiation tolerance.

In this paper we present the statistics of $V_{\rm th}$ loss for NROM single memory cells after irradiation with photons and ions. Results of memory discharge during irradiation in the active mode (read voltage applied) are also reported.

II. EXPERIMENTAL

NROM cells fabricated by TowerJazz (microFlash process flow) had channel dimensions of $W \times L = 0.18 \times 0.42\ \mu\mathrm{m}^2$. One bit per cell was programmed by applying gate voltage (V_G) of 9 V and drain voltage (V_D) of 4 V for 10 μs. Source voltage (V_S) was 0 V Erase was achieved by applying $V_D = 9$ V and $V_S = 3$ V, at $V_G = 0$ V for 50 ms. Read-out was performed at $V_{\rm DS} = 1.8$ V. The $V_{\rm th}$ was measured at the drain current (I_{DS}) of 1 μA.

In the passive mode experiments, wafer level devices were irradiated at room temperature in dark conditions with floating electrodes using either γ- or X-ray photons or high energy ions (B, Br and Au). The ion energies were chosen to introduce the implanted ions (B, Br, and Au) deep into the Si substrate, beyond the device active part. The ion irradiation total fluence, measured in $\mathrm{ions/cm^2}$, was converted into absorbed dose evaluated in rad(Si) [4] to directly compare the different irradiation conditions. The conversion dose/rad(Si) was made using the linear energy transfer (LET) values reported in Table I and it did not consider the columnar recombination effect observed in dielectrics after irradiation [8], [9]. All the irradiation details are summarized in Table I.

To guarantee statistically significant results at least 10 memory cells were studied for each of the doses and types of irradiation. Each die underwent a single irradiation; different doses were performed on different dies. A total of $\sim$1000 samples were investigated. All cells were fully characterized before and after the irradiation. Each set of cells (ten devices) is in the same die and most of the dies come from the same wafer. In any case all the dies are from the same diffusion lot.

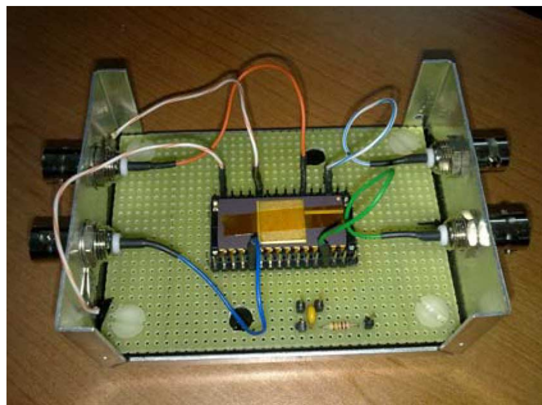

Fig. 4. Picture of the board (mini-Dom) used for "in-situ" measurements.

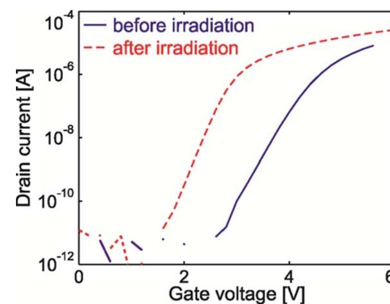

Fig. 5. Drain-source current as a function of the gate voltage for a programmed cell before (blue solid line) and after (red dashed line) irradiation with $1 \times 10^{10}\ \mathrm{B/cm^2}$, corresponding to $\sim 580\ \mathrm{krad(Si)}$.

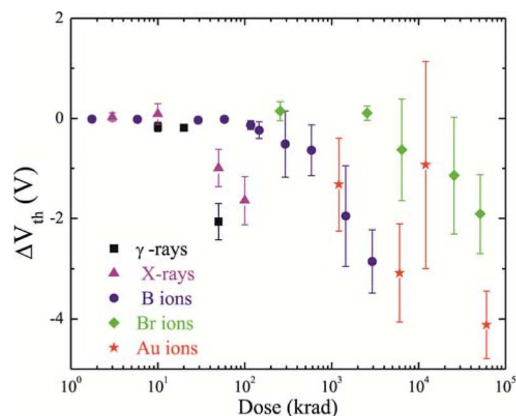

Fig. 6. Averaged threshold voltage shift as a function of the log of the irradiation dose for: γ-rays (black squares); X-rays (magenta triangles); B (blue circles); Br (green diamonds) and Au (red stars) irradiations.

Active mode experiments were performed using a board fabricated to this purpose and shown in Fig. 4. The dies with NROM single cells were assembled in 28 pin packages which allowed connecting 10 devices to the pins. The package lid was removed to allow direct irradiation of the device region. The single cells were selected by addressing the pins connected to the BNC plugs. The mini-chuck (named mini-Dom) was closed with an Al lid, not shown in the picture, having an opening above the device region. The device region is below the yellow square cap in Fig. 4. In this way only the die was directly hit by the radiation flux and all the cables and electronics were shielded. Voltages $V_D = 1.8$ V and V_G values in the range of 3–4 V for programmed bits, defined in order to measure a point in the subthreshold region, were applied to the programmed devices when reading the $I_{\rm DS}$ current.

III. Results and Discussion

The main degradation effect in NROM at irradiation doses below 100 krad(Si) is charge trapping in the memory stack. The ionizing radiation generates high energy electron/hole pairs in the dielectric but, on the average, holes are trapped by silicon nitride or oxide traps while electrons escape the dielectric stack [8]. At irradiation doses above 100 krad(Si), permanent defects may be created in the oxide layers, leading to the formation of clusters of traps that can act as percolation paths across the dielectrics. These effects are especially pronounced in the ONO bottom oxide where even one trap in the middle of 5 nm bottom oxide may result in a percolation path (leakage channel).

The effects of irradiation were observed by monitoring $V_{\rm th}$ before $\left(V_{\rm th}^i\right)$ and after $\left(V_{\rm th}^f\right)$ irradiation. An example of $V_{\rm th}$ shift after irradiation is shown in Fig. 5 (dashed red line) in the case of 10 MeV B irradiation to a dose of $\sim 580\ \mathrm{krad(Si)}$ (see Table I).

The shift indicates a partial compensation of the electron charge at nitride traps. The $V_{\rm th}$ shift $\Delta V_{\rm th} = V_{\rm th}^f - V_{\rm th}^i$ was recorded as a function of the total irradiation dose in all the experiments performed. The results for programmed cells are summarized in Fig. 6. Two main features are immediately observed regardless of the irradiation source: i) the average $|\Delta V_{\rm th}|$ increases with the irradiation dose; ii) a noticeable $\Delta V_{\rm th}$ dispersion is observed for all the experiments and it increases with the dose.

To better understand the statistics of the charge loss (ΔV_{th}), the standard deviation $(\sigma_{\Delta \rm Vth})$ of ΔV_{th} was plotted as a function of the average $\Delta V_{th}(\mu_{\Delta Vth})$ for all the experiments we carried out and the results are shown in Fig. 7 for programmed bits. The data indicates a unique trend: linear dependency in a log-log scale. The linear fit, shown by a solid line, has a slope of $\sim 2.1 \pm 0.4$ suggesting that the average (μ) and the standard deviation (σ) of the threshold voltage shift are related as:

$$\mu_{\Delta Vth} \cong 2.1 \sigma_{\Delta Vth} \tag{1}$$

Though for each single radiation type the statistics is not very high, numerous sets of radiation sources and doses spanning over many decades demonstrate that all the measurement points fall onto the same line. Equation (1) holds regardless of the amount of stored charge, radiation type and dose. The data, therefore, strongly suggest that a common physical phenomenon could explain the observed trend.

It is well known that the ionizing radiation damage is randomly distributed in the gate dielectrics. An example of random process of this sort is the oxide dielectric breakdown [10], [11], well described by the Weibull distribution [12]. Radiation degradation can also be considered a random process with

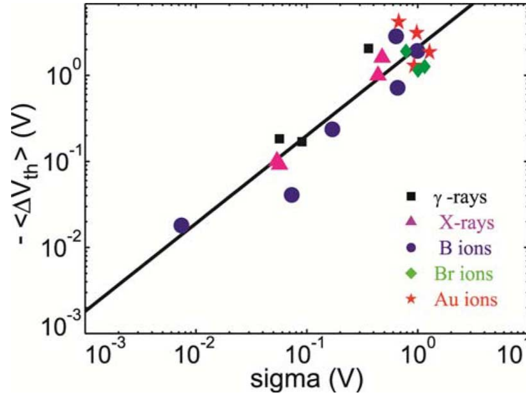

Fig. 7. Averaged threshold voltage shift as a function of the dispersion in programmed bits after irradiation with: γ-rays (black squares); X-rays (magenta triangles); B (blue circles); Br (green diamonds) and Au (red stars) irradiations.

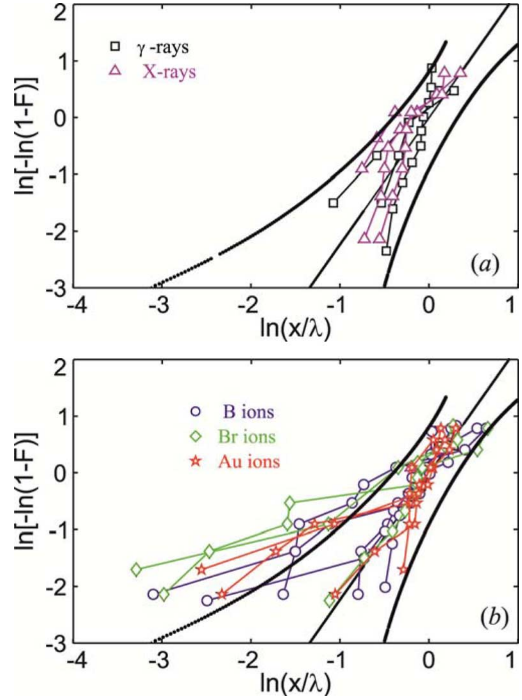

Fig. 8. Weibull function for $k = 2.2$ (solid black line) for all the experiments performed (a) with photons: γ-rays (black squares) and X-rays (magenta triangles); (b) with ions: B (blue circles); Br (green diamonds) and Au (red stars) irradiations. The black curves on the both sides of Weibull function indicate the 95% confidence level [14].

"weakest links" resulting in V_{th} loss above the allowed margins [13]. The ionizing radiation will produce holes which either discharge the trapped electrons or are captured on defects and therefore locally compensate the charge of the trapped electrons. For each discharged or compensated electron, we consider $\Delta V_{th} = N^{*}\Delta V_{th0}$ where N is the number of discharged, or compensated, electrons and ΔV_{th0} is q/C_{self}, where q is the elementary charge and C_{self} is the self-capacitance of the storage defect. Then, if the NROM array is subjected to an irradiation to a dose D_0, each of the cells will have a ΔV_{th}, and we expect $F(\Delta V_{Th}) = 1 - \exp\left[-(\Delta V_{th}/\lambda)^k\right]$. Known the average and standard deviation of the distribution, (1) can be written as:

$$\Gamma\left(1+\frac{1}{k}\right) \approx 2.1 \cdot \sqrt{\Gamma\left(1+\frac{2}{k}\right) - \Gamma^2\left(1+\frac{1}{k}\right)} \quad (2)$$

where Γ is the gamma function defined as $\Gamma(z) = \int_0^{+\infty} t^{z-1}e^{-t}dt$, and k is the Weibull shape parameter. The condition expressed by (2) is satisfied only by $k \cong 2.2$ (numerically determined). We, therefore, conclude that even if the radiation source and irradiation conditions are drastically varied, in all cases the same k, i.e., Weibull distribution slope, should be observed.

In order to verify this hypothesis, the different collected data are compared using the same normalized scale (Fig. 8(a) and (b)). For this reason, for each data set we assumed a Weibull function having $k = 2.2$ and λ determined using the experimental mean value. The Weibull cumulative distribution can be represented by a weibit, hence a straight line by plotting $\ln|-\ln(1-F)|$ against $\ln(x/\lambda)$. In these coordinates, k is the slope. The Weibull distribution $F(x, \lambda, k)$ with $k = 2.2$ is presented as a solid straight line. The statistical confidence of our measurements (95%) is expressed by two curves on the both sides of $F(x, \lambda, k)$ [14]. All our data points follow quite well the proposed statistics for both photons (Fig. 8(a)) and ions (Fig. 8(b)). The analysis of irradiated single cells clearly shows that all the device sets, regardless of radiation source and dose, belong to the same Weibull distribution. This is direct evidence that all the results are ruled by the same physical mechanism.

V_{th} loss may be due to two possible mechanisms connected with hot holes generated by radiation: trapping of thermalized holes or creation of traps in the oxide layers.

In the first case the trapped holes compensate the electron charge stored in nitride traps. In the second case trap-assisted tunneling generated by defects can also result in progressive discharge of the stored electrons with the increasing of radiation dose. It is interesting that both mechanisms can be statistically described by a Weibull distribution with $k = 2$. This value is very close to 2.2 registered in our experiments [15]. The measurements performed so far do not allow us to distinguish between the two mechanisms but, the most important result is that we found the statistics ruling the mechanism.

Experiments, in the active regime (under read-out bias), performed on a programmed cell during irradiation clearly show that the I_{DS} current at a fixed gate voltage (V_G in the range 3–4 V) exhibits a "step-like" behavior. A typical example for X-rays irradiation is shown in Fig. 9. The data were acquired, in subthreshold regime, using a $V_{\mathrm{DS}} = 1.8$ V (read-out voltage) and $V_G = 3.5$ V in order to maximize each variation in the stored charge value. The dose rate is reported in Table I.

The same experiments were performed with light ions (B) and with γ-rays (not shown). The data reported in Fig. 10, refer to 10 MeV B irradiation to a dose rate of $10^8\ \mathrm{cm}^{-2}$ corresponding to $\sim 50\ \mathrm{krad(Si)}$ and were acquired using a $V_{\mathrm{DS}} = 1.8$ V (read-out voltage) and $V_G = 3.8$ V on a programmed bit. The beam was switched on after 20 seconds and switched off after 580 s.

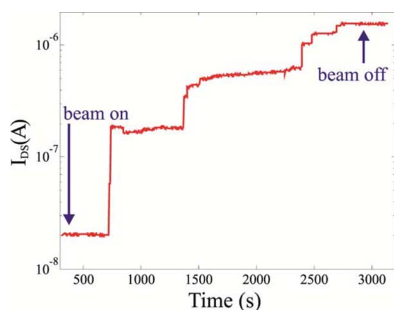

Fig. 9. Drain-source current as a function of the irradiation time for a programmed sample during X-rays irradiation (3.9 rad(Si)/s). The arrows indicate the beam on and beam off points. During irradiation $V_G = 3.5$ V, $V_{DS} = 1.8$ V.

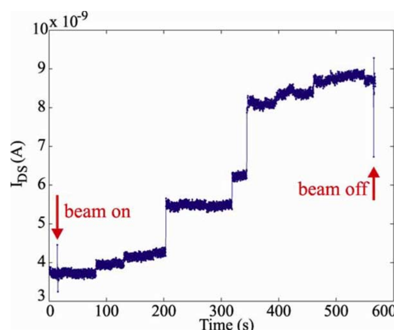

Fig. 10. Drain-source current as a function of the irradiation time for a programmed cell during 10 MeV B irradiation (50 krad(Si)/s). During irradiation $V_G = 3.8$ V, $V_{DS} = 1.8$ V.

The figure shows a step-like behavior of the drain-source current also in this case. Hence a result similar to the one just described for photon irradiation: I_{DS} increases by steps.

It is known that the charge is stored in point-defects lying in the nitride layer [5] and that each charge produces an electrostatic field within the Debye length The presence of steps in the I_{DS}, could be explained assuming single electron discharge and/or compensation events occurring at the programmed bit [16]. The area influenced by an electron is obviously smaller than the whole channel area, hence one electron loss (or gain) leads to a local variation of the V_{th}. As a result, the jumps experimentally observed in the drain-source current are ascribable to modifications in the percolation paths over the channel area joining source and drain. The observed dispersion in the measured step size may be attributed to a statistically changing percolation path [16].

IV. Conclusion

In summary, our results indicate that the V_{th} loss in NROM memory devices due to ionizing radiation exhibits fluctuations well explained by a Weibull statistics with a $k \sim 2.2$ shape parameter regardless of the irradiation species, including photons of different energies (γ- and X-rays), light (Boron) and heavy (Br and Au) ions, and regardless of the total dose ranging from few krad(Si) to ~ 60 Mrad(Si). The Trapping of thermalized holes or the creation of defect traps in the NROM oxide layers causes to V_{th} loss.

The knowledge of the discharging mechanism statistics could allow one to implement a memory reprogramming algorithm to improve the radiation tolerance of a memory array. Our findings provide also an even more important statement: since different irradiation sources are ruled by the same, within the experimental errors, discharge statistics, only one algorithm must be implemented to improve the system tolerance.

Finally, I_{DS} measurements in-situ during irradiation shows that the memory discharge occurs in steps, regardless of the irradiation source used.

References

[1] G. Cellere, A. Paccagnella, A. Visconti, and M. Bonanomi, "Ionizing radiation effects on floating gates," *Appl. Phys. Lett.*, vol. 85, no. 3, pp. 485–487, 2004.

[2] A. Gasperin, A. Cester, N. Wrachien, A. Paccagnella, V. Ancarani, and C. Gerardi, "Radiation-Induced modifications of the electrical characteristics of nanocrystal memory cells and arrays," *IEEE Trans. Nucl. Sci.*, vol. 53, no. 6, pp. 3693–3700, Dec. 2006.

[3] M. Lisiansky, G. Cassuto, Y. Roizin, D. Corso, S. Libertino, A. Marino, S. A. Lombardo, I. Crupi, C. Pace, F. Crupi, D. Fuks, A. Kiv, E. D. Sala, G. Capuano, and F. Palumbo, "Radiation tolerance of NROM embedded products," *IEEE Trans. Nucl. Sci.*, vol. 57, no. 4, pp. 2309–2317, Aug. 2010.

[4] S. Libertino, D. Corso, G. Murè, A. Marino, F. Palumbo, F. Principato, G. Cannella, T. Schillaci, S. Giarusso, F. Celi, M. Lisiansky, Y. Roizin, and S. Lombardo, "Radiation effects in nitride read-only memories," *Microelectr. Rel.*, vol. 50, pp. 1857–1860, Aug. 2010.

[5] B. Eitan, P. Pavan, I. Bloom, E. Aloni, A. Frommer, and D. Finzi, "NROM: A novel localized trapping 2-bit nonvolatile memory cell," *IEEE Electron Device Lett.*, vol. 21, pp. 543–545, Nov. 2000.

[6] A. Shappir, D. Levy, Y. Shacham-Diamand, E. Lusky, I. Bloom, and B. Eitan, "Spatial characterization of localized charge trapping and charge redistribution in the NROM device," *Solid State Electr.*, vol. 48, pp. 1489–1495, Apr. 2004.

[7] P. J. McWhorter, S. L. Miller, and T. A. Dellin, "Radiation response of SNOS nonvolatile transistors," *IEEE Trans. Nucl. Sci.*, vol. NS-33, no. 6, pp. 1414–1419, Dec. 1986.

[8] T. R. Oldham, "Recombination along the tracks of heavy charged particles in SiO2 films," *J. Appl. Phys.*, vol. 57, pp. 2695–2702, Apr. 1985.

[9] T. R. Oldham and F. B. McLean, "Total ionizing dose effects in MOS oxides and devices," *IEEE Trans. Nucl. Sci.*, vol. 50, no. 3, pp. 483–499, Jun. 2003.

[10] J. H. Stathis, "Percolation models for gate oxide breakdown," *J. of App. Phys.*, vol. 86, no. 9, pp. 5757–5766, Nov. 1999.

[11] J. H. Stathis, "Reliability limits for the gate insulator in CMOS technology," *IBM J. Res. Dev.*, vol. 46, no. 2/3, pp. 265–286, Mar./May 2002.

[12] J. F. Lawless, *Statistical Models and Methods for Lifetime Data*. New York: Wiley, 1982.

[13] B. Wang, J. S. Suehle, E. M. Vogel, J. R. Conley, Jr, C. E. Weintraub, A. H. Johnston, and J. B. Bernstein, "Latent reliability degradation of ultra-thin oxides after heavy ion and γ-ray irradiation," in *Proc. IEEE Integrated Reliability Workshop*, 2001, pp. 16–19.

[14] J. Jacquelin, "Inference of sampling on Weibull representation," *IEEE Trans. Electr. Dev.*, vol. 3, no. 6, pp. 806–808, Dec. 1996.

[15] D. Corso, S. Libertino, M. Lisiansky, Y. Roizin, F. Palumbo, F. Principato, C. Pace, P. Finocchiaro, and S. Lombardo, "Threshold voltage variability of NROM memories after exposure to ionizing radiation," *IEEE Trans. Electr. Dev.*, vol. 50, no. 10, pp. 2597 –2602, 2012.

[16] D. Corso, C. Pace, F. Crupi, and S. A. Lombardo, "Single-Electron program/erase tunnel events in nanocrystal memories," *IEEE Trans. Nanotechn.*, vol. 6, no. 1, pp. 35–42, Jan. 2007.